

Finite-temperature magnetism of FeRh compounds

S. Polesya,^{*} S. Mankovsky,[†] D. Ködderitzsch, J. Minár, and H. Ebert

Department Chemie, Physikalische Chemie, Universität München, Butenandstr. 5-13, 81377 München, Germany

(Received 23 September 2015; revised manuscript received 23 December 2015; published 28 January 2016)

The temperature dependent stability of the magnetic phases of FeRh were investigated by means of total energy calculations with magnetic disorder treated within the uncompensated disordered local moment approach. In addition, Monte Carlo simulations based on the extended Heisenberg model have been performed, using exchange coupling parameters obtained from first principles. The crucial role and interplay of two factors in the metamagnetic transition in FeRh has been revealed, namely the dependence of the Fe-Fe exchange coupling parameters on the temperature-governed degree of magnetic disorder in the system and the stabilizing nature of the induced magnetic moment on Rh-sites. An important observation is the temperature dependence of these two competing factors.

DOI: [10.1103/PhysRevB.93.024423](https://doi.org/10.1103/PhysRevB.93.024423)

I. INTRODUCTION

FeRh with composition close to being equiatomic crystallizes in the CsCl structure and exhibits rather interesting magnetic properties attractive for investigation for various reasons. It is antiferromagnetically (AFM) ordered in the ground state and reveals a first-order metamagnetic transition to the ferromagnetic (FM) state at $T_m \approx 340\text{--}350$ K [1]. A transition to a paramagnetic (PM) state occurs at $T_C = 675$ K [1]. It is worth noting that the temperature of the metamagnetic transition is very sensitive to the conditions of sample preparation. Despite several attempts to shed light on the physical origin of the magnetic properties of FeRh-based alloys, both within experimental [2–4] and theoretical [5–13] investigations, they are still under debate.

Various mechanisms have been suggested to explain the driving force for the AFM-FM transition. The early model suggested by Kittel [14], namely the exchange-interaction-inversion model, associated the AFM-FM phase transition with the dominant role of the change of magnetoelastic energy. More recent investigations, however, demonstrated a minor role of the exchange magnetoelastic energy [15].

The experimentally observed large change of the entropy, i.e., 14.0 mJ/g/K [15] or 12.58 mJ/g/K [16], is mainly attributed to the electronic contribution related to spin fluctuations on the Rh atoms. This observation implies a key role of the Rh induced magnetic moments for the stabilization of the FM state [16–18]. This idea was supported by theoretical investigations based on first-principles electronic structure calculations [3,5–7,10,12].

So far there is no clear understanding of the finite temperature magnetic properties of FeRh when small amounts of impurities are present [15,19–21]. Recent first-principles investigations by Staunton *et al.* [12], based on the analysis of the electronic entropy highlights the impact of small compositional changes on the temperature of the metamagnetic transition.

The reversibility of this transition and the small relaxation time makes it attractive for applications. Transport measurements demonstrate a strong drop of the electrical resistivity

during the metamagnetic phase transition [16,22] from the AFM to the FM state. As the metamagnetic transition can be manipulated by an external magnetic field, this feature of the resistivity leads to a giant magnetoresistance phenomena in the system around T_m , that makes FeRh an appealing material for future data storage devices [13,23].

II. COMPUTATIONAL DETAILS

Within the present study spin-polarized electronic structure calculations have been performed using the fully relativistic multiple scattering Korringa-Kohn-Rostoker (KKR) Green function method [24,25]. All calculations have been performed in full-potential (FP) mode. Density functional theory employing the generalized gradient approximation (GGA) was used with the parametrization of the exchange-correlation potential as given by Perdew, Burke, and Ernzerhof (PBE) [26]. For the angular momentum expansion of the Green function a cutoff of $\ell_{\max} = 3$ was applied. For determining configurational averages in substitutionally disordered alloys, the self-consistent coherent potential approximation (CPA) method was employed. The magnetic disorder in the DFT calculations for systems in the paramagnetic (PM) state ($T > T_C$) was treated within the disordered local moment (DLM) method. To simulate the temperature induced partial magnetic disorder below the Curie temperature, the so-called uncompensated Disordered Local Moment (uDLM) approximation (see, e.g., Ref. [27]) was used. In this case the Fe subsystem was represented by the pseudoalloy $\text{Fe}_{1-x}^{\uparrow}\text{Fe}_x^{\downarrow}$ with Fe sites occupied by two-components Fe^{\uparrow} and Fe^{\downarrow} with the opposite directions of magnetic moment, “up” and “down”, respectively, and x varying in the interval [0.0,0.5].

The finite temperature magnetic properties have been investigated via Monte Carlo (MC) simulations based on the extended Heisenberg model, using a standard Metropolis algorithm [28,29]. The exchange coupling parameters J_{ij} for these calculations were obtained using the expression given by Lichtenstein [30,31].

III. RESULTS

The calculated total energies of the FM and AFM states of FeRh as a function of the lattice parameter, represented in

^{*}Svitlana.Polesya@cup.uni-muenchen.de

[†]Sergiy.Mankovsky@cup.uni-muenchen.de

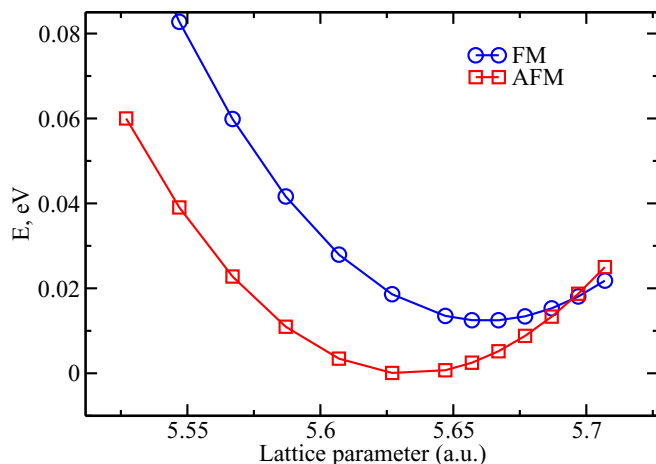


FIG. 1. Total energy calculated for the FM and AFM states of FeRh as a function of the lattice parameter a

Fig. 1, are in full agreement with the experimental results as well as with calculations of others authors [6,32]. The energy minimum for the AFM state for the lattice parameter $a = 5.63$ a.u. is about 17 meV lower than that for the FM state occurring at $a = 5.66$ a.u. Thus, the AFM-FM transition should be accompanied by a lattice expansion with a magnetovolume effect of 1.6% which slightly overestimates the value observed experimentally, 1% [18].

The Fe magnetic moment obtained for the energy minimum in the FM state is $3.3 \mu_B$, which is in line with the neutron scattering measurements giving $3.0 \mu_B$ per Fe atom [33]. Its magnitude remains almost unchanged in the AFM ground state ($3.2 \mu_B$). The induced total magnetic moment on the Rh atomic sites calculated for the FM state is equal to $1.0 \mu_B$ and vanishes in the AFM state.

The density of states (DOS) curves for the FM, AFM and DLM states are shown in Fig. 2(a), 2(b), 2(c), respectively. Only a weak dependency on the volume is observable for the DOS calculated for the FM (a) and AFM (b) states. In the FM state a strong spin-dependent hybridization of Rh states is apparent [Fig. 2 (a)], which leads to the formation of a magnetic moment of $1 \mu_B$ on the Rh atomic site. In the AFM state the Rh DOS for the majority- and minority-spin states are identical due to symmetry, resulting in a Rh magnetic moment equal to $0 \mu_B$. The Rh-related electronic states for both of the DOS spin channels in these cases exhibits hybridization with Fe minority-spin states (essentially, above the Fermi energy) and majority-spin states (below the Fermi energy), in line with the discussion by Sandratskii and Mavropoulos [7]. This demonstrates that in the AFM state the vanishing total magnetic moment on the Rh site is a result of the hybridization-governed redistribution of spin density and not because of vanishing spin density within the Rh atomic site.

Note also, that the Rh DOS at the Fermi level is rather small and, therefore, a pronounced Stoner enhancement of the magnetic moment induced on Rh can be ruled out. Thus, as will be also discussed below, the large Rh magnetic moment in the FM state should be attributed to a strong spin-dependent hybridization.

As the AFM-FM transition occurs at finite temperature it is necessary to take into account the temperature induced

magnetic disorder in the system when comparing the total energies of the two states. For this reason the calculations have been performed accounting for magnetic disorder treated within the uDLM approximation. For the system under discussion, the parameter x describing the degree of magnetic disorder can be represented within this approach in terms

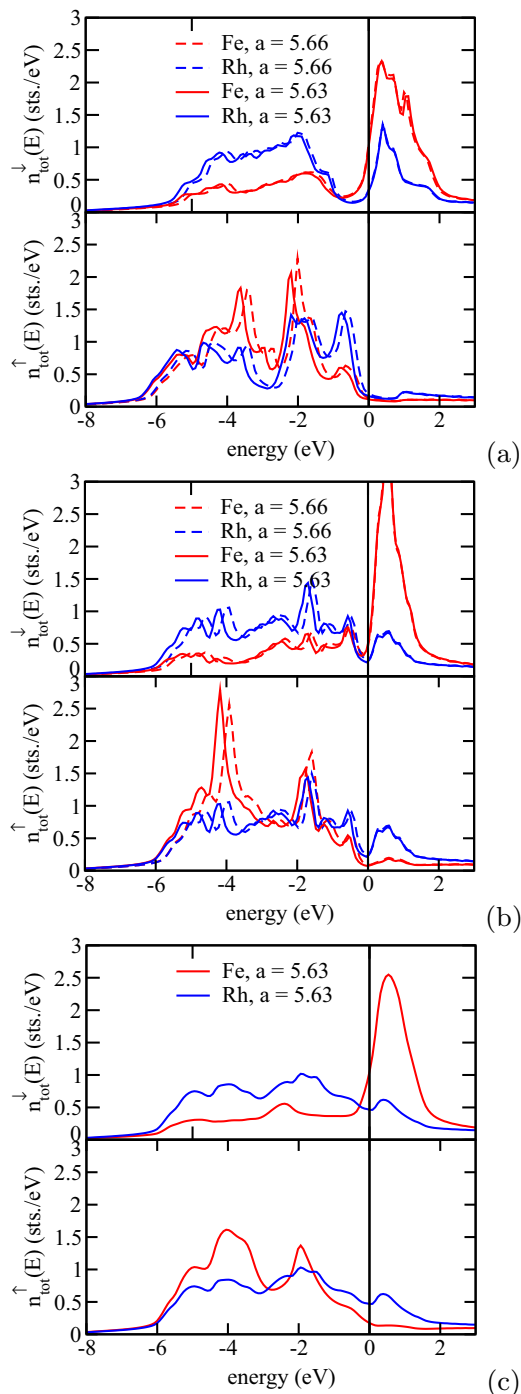


FIG. 2. Density of states for the FM state (a), AFM state (b), and random-spin state treated within the DLM approach (c). The solid and dashed lines in (a) and (b) represent the results for FeRh with the lattice parameters corresponding to the minimum of total energy for the AFM state (solid line, $a = 5.63$ a.u.) and FM state (dashed line, $a = 5.66$ a.u.)

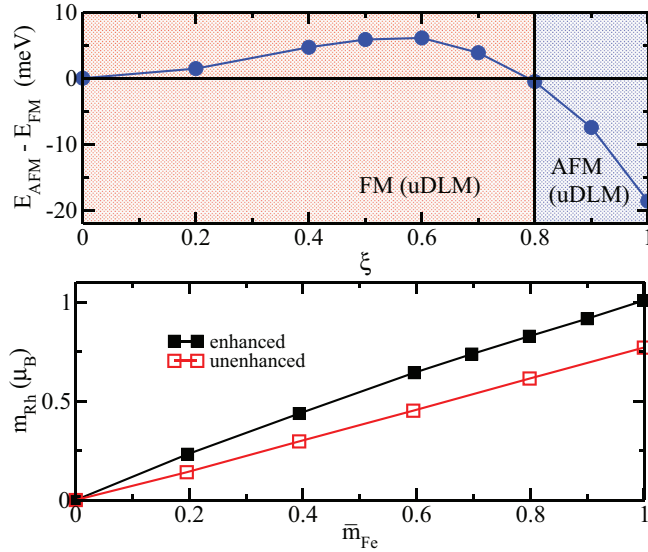


FIG. 3. Top: Difference between the total energies, $E_{AFM} - E_{FM}$ as a function of ξ , obtained by uDLM calculations for the FeRh compound having FM and AFM magnetic order, with lattice parameters corresponding to the total energy minimum in the AFM state, $a = 5.63$ a.u. Bottom: Enhanced and non-enhanced magnetic moment on the Rh-site in the FM (uDLM) state, as a function of the order parameters average normalized magnetic moment on Fe sites, \bar{m}_{Fe} .

of the order parameter ξ . In the case of the FM state with partial magnetic disorder, the order parameter is given by the normalized average magnetic moment per Fe atom $\xi = \bar{m}_{Fe} = \langle M_{Fe} \rangle / M_{Fe} = (M_{Fe}(1-x) - M_{Fe}x) / M_{Fe} = (1-2x)$. On the other hand, in the case of the partially disordered AFM state the order parameter can be represented as $\xi = \frac{1}{2}[(\langle M_{Fe}^{\uparrow} \rangle - \langle M_{Fe}^{\downarrow} \rangle) / |M_{Fe}|] = (1-2x)$, where $\langle M_{Fe}^{\uparrow} \rangle$ and $\langle M_{Fe}^{\downarrow} \rangle$ are the average magnetic moments of Fe sublattices having opposite orientation with respect to each other, while the total magnetic moment is equal to $0 \mu_B$ for each ξ value.

Figure 3 shows the total energy difference $E_{AFM} - E_{FM}$ as a function of ξ for FeRh with the lattice parameter $a = 5.63$ a.u. corresponding to the energy minimum of the AFM state. At $\xi = 1$, the difference is negative, demonstrating the stability of the AFM state in line with the results shown in Fig. 1. An increase of the disorder represented by a decrease of ξ leads to a decrease of stability of the AFM state such that at $\xi \leq 0.8$ the FM state becomes more stable up to the fully disordered state with $\xi = 0$, when both types of magnetic order, FM and AFM, have the same energy. The Rh magnetic moment in the case of FM order (Fig. 3, bottom) exhibits almost a linear dependence on ξ changing from $M_{Rh} = 0.0 \mu_B$ in the fully disordered DLM state to $M_{Rh} = 1.0 \mu_B$ in the ordered FM state.

In summary, these results demonstrate the following effects of increasing magnetic disorder: (i) a stabilization of the FM state with respect to the AFM state and (ii) the stability of the FM state is a result of the decrease of the Rh magnetic moment.

Therefore, when discussing the driving forces behind the metamagnetic AFM-FM phase transition, other additional effects than just the magnetization of the Rh sublattice have

to be considered. This has already become apparent within various investigations [5–8, 11–13]. Below we will investigate the features of the interatomic exchange interactions to demonstrate their crucial role for the AFM-FM phase transition.

First we discuss some features of the Rh magnetic moment which are related to the magnetic disorder in the system. The magnetic moment of Rh is induced by a spin dependent hybridization of its electronic states with the electronic states of surrounding Fe atoms. This hybridization plays a crucial role during the transition from the FM to the AFM state. To demonstrate the strong covalent character of the Rh magnetism, SCF calculations have been performed by suppressing for the spin-dependent part of the exchange-correlation potential ($B_{xc}^{Rh} = 0$) that is responsible for an enhancement of the spin magnetic moment induced by the hybridisation with the Fe states. Figure 3 (open symbols) shows that the non-enhanced Rh magnetic moment is only $\sim 25\%$ smaller than the proper one. The same is observed for the total energy. This demonstrates the significant role of the spin dependent hybridization for the formation of a large magnetic moment on the Rh site. As a result, the varying magnetic disorder in the Fe sublattice in the presence of the weak Rh exchange enhancement leads to an almost linear change of M_{Rh} as a function of \bar{m}_{Fe} .

To investigate the stability of the FM and AFM ordered magnetic states at finite temperature the exchange coupling parameters J_{ij} have been calculated for different reference states: AFM, FM, and DLM. These interactions can be seen to map the magnetic energy of the system onto the Heisenberg Hamiltonian accounting for the bilinear interatomic exchange terms. The corresponding results are presented in Fig. 4.

Discussing these results, it is convenient to distinguish between the two Fe sublattices with opposite directions of the magnetic moments in the AFM state. For each Fe atom its first and third neighbor in the Fe subsystem belongs to another sublattice. One can see that for all reference states the exchange couplings with these neighbors are negative indicating the trend towards the formation of AFM order. The interaction with the third Fe neighbor depends only weakly on the reference state, while the interactions with the first neighbor are close to 0 meV in the case of FM reference state and is about -8.0 meV for the AFM state. Since the Rh magnetic moment in the AFM state is equal to $0 \mu_B$, it does not contribute to the magnetic energy. As a consequence only the Fe-Fe exchange interactions are responsible for the stabilization of this state. In contrast to this situation, the FM order in the system can be stabilized by a rather strong Fe-Rh interaction since the Rh magnetic moments are non-zero, giving a negative contribution to the magnetic energy competing with the positive one due to the Fe-Fe interatomic exchange. Thus, the transition from the AFM to FM state is essentially a result of the competition of these interactions.

Thus, the behavior of the FM and AFM energy variation shown in Fig. 3 and demonstrating the stabilization of the FM state upon increase of the magnetic disorder, can be attributed to the modification of the Fe-Fe exchange coupling parameters, in particular, to a strong decrease of the AFM interactions with the first neighbors. In the DLM state the situation is very different. The Fe-Fe exchange interactions are rather close to those obtained for the FM state, but the Rh magnetic moments

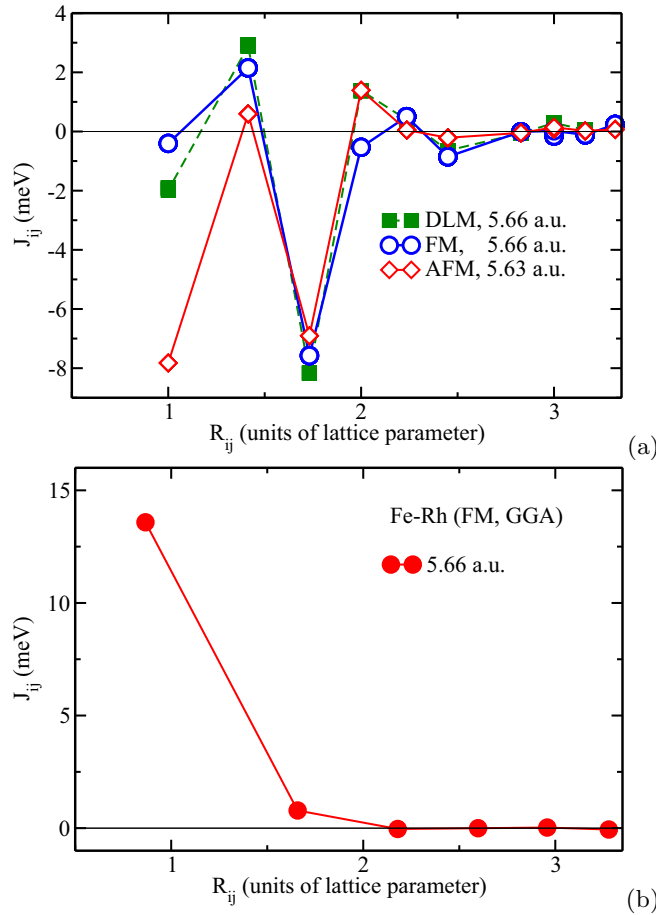


FIG. 4. (a) The Fe-Fe interatomic exchange coupling parameters calculated for the FM (open circles), AFM (open diamonds), and DLM (squares) states; (b) the Fe-Rh exchange coupling parameters calculated for the FM state (the Rh magnetic moment is $m \approx 1 \mu_B$).

are equal to zero and therefore give no contribution to the magnetic energy.

Two remarks concerning the approximations used for the calculations are in due place concerning the Monte Carlo simulations. The conventional Heisenberg Hamiltonian should be generalized beyond the classical form: (i) in order to account for the contribution due to induced Rh magnetic moments; (ii) to account for not only bilinear terms of the magnetic energy expansion but also for terms of higher order. The second generalization is required since the insufficient conventional dipolar form of the Hamiltonian gets appreciable corrections from bilinear exchange coupling parameters calculated for different reference states. The general form of the expansion of magnetic energy around a reference state may therefore be represented as follows (see, e.g., [34–36])

$$\begin{aligned}
 E &= E_{\text{ref}} + \Delta E(|M_i|) - \sum_{ij} J_{ij}^{(2)}(\hat{\mathbf{e}}_i \cdot \hat{\mathbf{e}}_j) \\
 &- \sum_{v=2}^n \sum_{ij} J_{ij}^{(2),(v)}(\hat{\mathbf{e}}_i \cdot \hat{\mathbf{e}}_j)^v - \frac{1}{4!} \sum_{ijkl} J_{ijkl}^{(4)}[(\hat{\mathbf{e}}_i \cdot \hat{\mathbf{e}}_j)(\hat{\mathbf{e}}_k \cdot \hat{\mathbf{e}}_l) \\
 &+ (\hat{\mathbf{e}}_j \cdot \hat{\mathbf{e}}_k)(\hat{\mathbf{e}}_l \cdot \hat{\mathbf{e}}_i) + (\hat{\mathbf{e}}_l \cdot \hat{\mathbf{e}}_i)(\hat{\mathbf{e}}_j \cdot \hat{\mathbf{e}}_k)] - \dots, \quad (1)
 \end{aligned}$$

where $\Delta E(|M_i|)$ is the change in energy due to the change of absolute values of local spin magnetic moments. This can be reduced to the conventional form of the Hamiltonian with redefined bilinear exchange interaction parameter \tilde{J} :

$$H_{\text{ext}} = - \sum_{\text{Fe};i,j} \left[\tilde{J}_{ij}^{\text{Fe-Fe}}(\bar{m}) + \sum_{\text{Rh};k} \tilde{J}_{ik}^{\text{Fe-Rh}} \chi_{kj} \right] (\mathbf{M}_i \cdot \mathbf{M}_j). \quad (2)$$

The first term in Eq. (2) characterizes the bilinear Fe-Fe transverse-fluctuation exchange energy with i, j indicating sites on the Fe sublattice.

The exchange coupling parameters defined in this case as $\tilde{J}_{ij}^{\text{Fe-Fe}} = \frac{\partial^2 \langle H \rangle}{\partial M_i \partial M_j}$, with $\langle \dots \rangle$ standing for the thermal average (see, e.g., [37]), can be calculated within the DLM approach based on the DFT Hamiltonian. The directions of the magnetic moments \mathbf{M}_i and \mathbf{M}_j are assumed to be collinear and aligned along the direction of the total magnetic moment. A modification of the electronic structure due to an increase of magnetic disorder for rising temperatures results in turn in a temperature dependence of the interatomic exchange interactions. On the other hand, evaluating the thermal average for the Heisenberg Hamiltonian in its extended form, Eq. (1), and using it in the expression for $\tilde{J}_{ij}^{\text{Fe-Fe}}(T)$, one can get the finite temperature exchange parameters in terms of the parameters of the Heisenberg model given by Eq. (1). As a result, one can see explicitly that they are determined by the bilinear exchange parameters $J_{ij}^{\text{Fe-Fe}}$ as well as by the higher order terms of the extended Heisenberg Hamiltonian, e.g., $\sum_{kl} J_{ijkl}^{(4)} \langle (\hat{\mathbf{e}}_k \cdot \hat{\mathbf{e}}_l) \rangle$, etc. Accounting for higher order terms results this way in the dependence of $\tilde{J}_{ij}^{\text{Fe-Fe}}$ parameters on the magnetic order in the system and as a consequence on the temperature.

The second term in Eq. (2) describes the energy changes related to longitudinal spin fluctuations on the Rh atoms [10,38] with k numbering Rh sublattice sites. Accounting for Rh magnetic moment via linear response formalism it is derived as follows:

$$H^{\text{Fe-Rh}} = - \sum_{\text{Fe};k,j} \tilde{J}_{ik}^{\text{Fe-Rh}} (\mathbf{m}_k \cdot \mathbf{M}_i) \quad (3)$$

$$= - \sum_{\text{Fe};i,j} \tilde{J}_{ik}^{\text{Fe-Rh}} \left(\left[\sum_j \chi_{kj} \mathbf{M}_j \right] \cdot \mathbf{M}_i \right) \quad (4)$$

$$= - \sum_{\text{Fe};k,j} \left[\sum_{\text{Rh};k} \tilde{J}_{ik}^{\text{Fe-Rh}} \chi_{kj} \right] (\mathbf{M}_i \cdot \mathbf{M}_j). \quad (5)$$

The magnetic moments on the Fe site are denoted as $\mathbf{M}_{i(j)}$. Considering the DLM state as reference state the dependence on the average magnetic moment in the first term can be considered in linear approximation to have the following form:

$$\tilde{J}_{ij}^{\text{Fe-Fe}}(\bar{m}) = \tilde{J}_{ij}^{\text{DLM}} + [\tilde{J}_{ij}^{\text{FM/AFM}} - \tilde{J}_{ij}^{\text{DLM}}] \bar{m}. \quad (6)$$

The term characterizing the longitudinal contribution was discussed previously [38].

The response function χ_{kj} occurring in Eq. (2) describes the Rh magnetic moment induced by surrounding Fe atoms and is dependent on the orientation of their magnetic moments. A

linear approximation expressed by a constant χ_{kj} was used, that is based on the results above showing the almost linear dependence of induced Rh magnetic moment on the average magnetic moment in Fe subsystem (see Fig. 3). As the Rh magnetic moment occurs essentially due to the spin-dependent hybridization of the Rh electronic states with the electronic states of neighboring Fe atoms, it is represented in MC simulations through the average magnetic moment on the first Fe neighbor shell around the Rh atoms, leading to an approximate form for the susceptibility function [38]

$$\mathbf{m}^{\text{Rh}} = \sum_j \chi_{0j}^{\text{Rh-Fe}} \mathbf{M}_j = X^{\text{Rh-Fe}} \sum_j \mathbf{M}_j, \quad (7)$$

where the summation is performed over the magnetic moments \mathbf{M}_j corresponding to Fe atoms within the first-neighbor shell around the “non-magnetic” Rh atom on site $i = 0$.

It should be pointed out in addition that the same DLM reference state for both the re-scaled FM and AFM exchange interactions has been used. This means that the exchange interactions should change abruptly at the metamagnetic transition point that accounts for latent heat connected with the first-order phase transition.

One should mention that the approach described above is rather close to the one used recently by Barker and Chantrell [11]. These authors point out the crucial role of the biquadratic exchange interactions to describe the AFM to FM phase transition in FeRh. Thus, in their as well as the present work, additional terms in the Heisenberg Hamiltonian are required to make a correction to the bilinear Fe-Fe exchange interactions due to the change of the degree of magnetic order in the system. It should be noted, however that Barker and Chantrell [11] attribute the biquadratic exchange interactions to the Fe-Rh-Fe type of exchange, referring to the calculations of Mryasov [10]. In the present work, the temperature dependence of the Fe-Fe exchange parameters is attributed primarily to the temperature dependent behavior of delocalized sp -electrons responsible for the indirect Fe-Fe exchange interactions. This dependence is accounted for by explicit calculations of the $\tilde{J}_{ij}^{\text{Fe-Fe}}$ parameters using the approach described above. We demonstrate also a linear dependence of the Rh magnetic moment on the magnetization of the Fe sublattice that allows to describe the Fe-Rh-Fe exchange interactions using the second term in Eq. (2).

To investigate the magnetic properties of FeRh-based systems at finite temperatures, Monte Carlo (MC) simulations have been performed based of the model Heisenberg Hamiltonian given in Eq. (2). Periodic boundary conditions have been used with the MC cell containing $L \times L \times L$ number of FeRh unit cells. Several sets of calculations have been performed for $L = 6$ to 10. Only the directions of the Fe moments (in the case of substitution of Fe by Ni atoms also the Ni moments) are considered as independent degrees of freedom. For the sequential update the Metropolis algorithm has been used. After each rotation of a Fe magnetic moment the induced moments on the neighboring Rh atoms are calculated, which in turn depend on the magnetic configuration of the surrounding Fe atoms. The total change of the energy due to both types of changes was accounted for the configuration

update. Up to 5000 MC steps (including trial rotations for all Fe atoms) have been used to reach the equilibrium and further 50 000–10 0000 MC steps—for computing averages. In the case of Ni substitution for Fe the results are in addition averaged over 10–20 random distribution of Fe and Ni atoms. For all sizes L used in the MC simulation the difference in AFM-FM transition temperature varied within ± 20 K without noteworthy changes for the other properties.

In a first step the calculations have been performed for the pure FeRh compound. The magnitude of the Fe magnetic moments have been fixed and only changes in orientation have been considered. On the other hand, the magnetic moments treated as induced magnetic moment according to Eq. (7), change their absolute value as well as the orientation depending on the orientations of the magnetic moments of the surrounding Fe atoms. At the same time, the total magnetic moment in the system can be rather small approaching $0 \mu_B$ at low (AFM state) and high (PM state) temperatures. Figure 5 shows the relative magnetization as a function of the temperature in comparison to experimental results. The calculated AFM-FM transition occurs at $T = 320$ K, rather close to the experimental value $T = 350$ K. As it was discussed above, it is caused by the increasing magnetic disorder in the system when the temperature increases. Two mechanisms are the major driving force for the transition. Firstly, the disorder-induced modification of the exchange coupling parameters. Secondly, the increase of the amplitude of randomly oriented fluctuations of the Rh magnetic moments in the AFM state due to increasing temperature-induced short-range FM order in the Fe subsystem [see Fig. 5(c)]. Therefore, it is the occurrence of magnetic moments on the Rh sites above a certain temperature that leads to a stabilization of the FM order in the system [see Fig. 5(d)]. A further temperature increase results in a decrease of the Rh magnetic moment, and to a transition to the PM state at $T = 720$ K. One has to stress the asymmetry of the metamagnetic transition in FeRh upon heating and cooling of the sample. This was demonstrated recently by a robust experimental investigation on the formation of FM and AFM phases. The authors concluded that the formation of the AFM phase upon a temperature decrease is dominated by a nucleation at defects in contrast to the formation of the FM phase for increasing temperature due to heterogeneous nucleation at different sites [39]. The latter results are in line with the present results of MC simulations [e.g., see Fig. 5(c),(d)]. However, different mechanism of nucleation upon cooling requires further generalization of the Hamiltonian and more sophisticated spin dynamics simulations to reproduce the temperature dependent behavior of magnetization in this case.

To investigate the influence of impurities on the metamagnetic transition, the calculations have been performed for the FeRh systems with 5 at.% and 10 at.% substitution of Fe by Ni atoms, and with 1 at.% and 2 at.% substitution of Rh by Fe atoms.

The presence of Ni impurities results in a decrease of the temperature of the metamagnetic transition. As one can see in Fig. 5(a), 5 and 10 at.% Ni in the Fe sublattice leads to transition temperatures of $T_m = 230$ and 180 K, respectively. The decrease of T_m is mainly governed by the difference in the Fe-Ni exchange interactions when compared to the Fe-

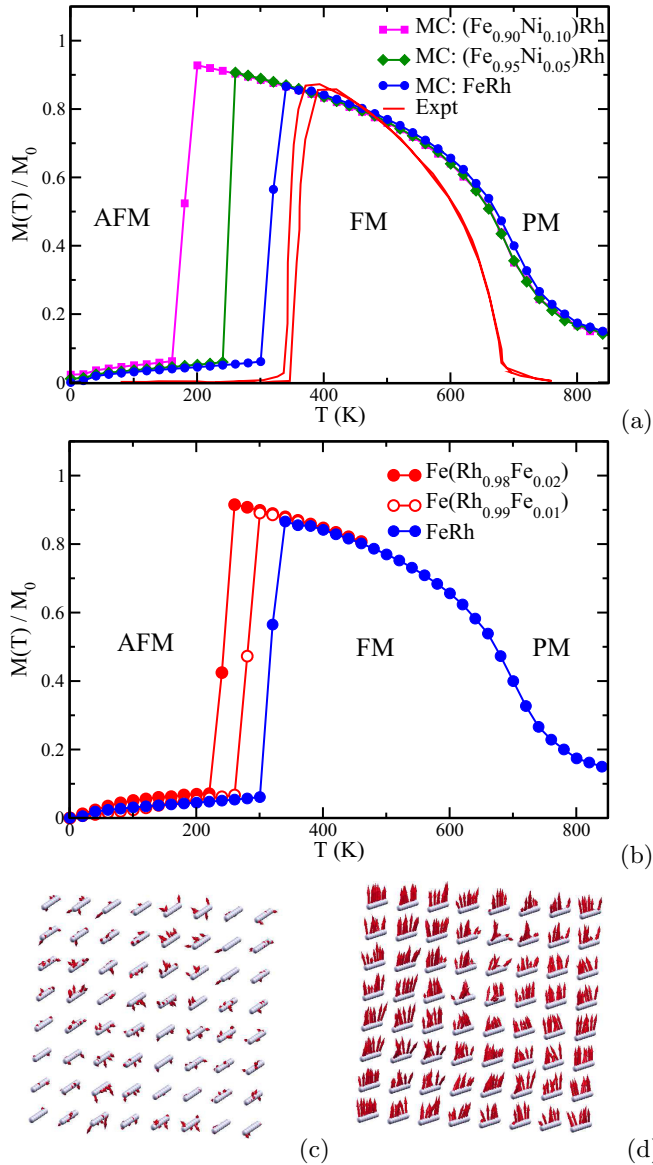


FIG. 5. Temperature dependent relative magnetization $M(T)/M_0$ (M_0 is the magnetization at $T = 0$ K) obtained within the MC simulations for $L = 8$: (a) $M(T)/M_0$ for pure FeRh (circles) in comparison with the experimental result; squares and diamonds represent the results for FeRh with 5 (diamonds) and 10 at. % (squares) substitution of Fe by Ni atoms; (b) $M(T)/M_0$ calculated for FeRh with 1 and 2 at. % of Fe (closed symbols) in the Rh sublattice, in comparison with the results for FeRh (open symbols). (c) and (d) show the induced magnetic moments on the Rh sublattice of pure FeRh at $T = 300$ and 340 K, respectively.

Fe exchange interactions. As one can see in Fig. 6, the Fe exchange interaction with the Ni atom at the first-neighbor position becomes positive. The Fe-Ni exchange interactions, when Ni occupies third-neighbor position, are negative but are much smaller in magnitude when compared to the Fe-Fe interactions. Both of these effects lead to a stabilization of the FM state, and as a consequence to a decrease of the temperature of metamagnetic AFM-FM transition.

Substitution of 1 and 2 atomic % of Rh by Fe atoms results in a decrease of the transition temperature from $T_m = 320$

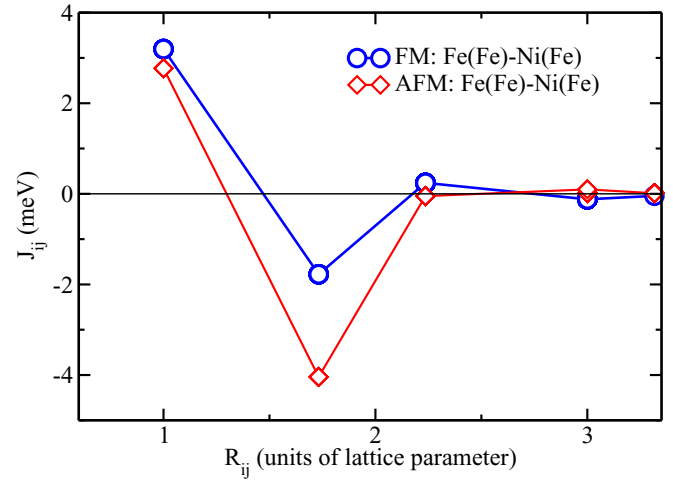


FIG. 6. (a) The Fe-Ni interatomic exchange coupling parameters calculated for the FM (open circles) and AFM (open diamonds) FeRh compound with 5 at. % substitution of Fe by Ni atoms: The Fe and Ni atoms correspond to different Fe sublattices having in the AFM state an opposite orientation of the magnetization.

to $T_m = 260$ and 220 K, respectively. In contrast to Fe substitution by Ni, the decrease of T_m is controlled by strong FM interactions between Fe atoms in the different (Fe and Rh) sublattices (see Fig. 7).

Thus, in line with experiment, for both types of impurities we have obtained a decrease of the temperature of the metamagnetic transition. On the other hand, the effect of impurities is much weaker than observed in experiment. This is clearly the result of approximations used in our calculations, in particular, for the exchange coupling parameters: (i) we use here the re-scaled bilinear exchange interactions in the model Hamiltonian, Eq. (2); (ii) the first-principles calculations of J_{ij} are performed for the collinear magnetic state at $T = 0$ K, which can be crucial for such a delicate system as FeRh. This problem can be avoided for example by the self-consistent

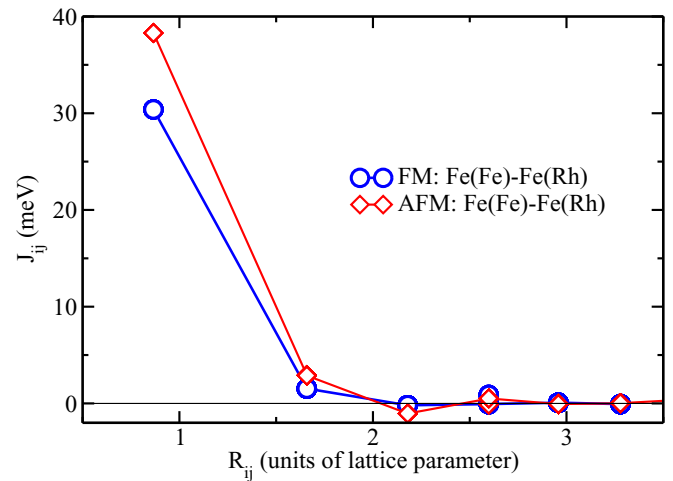


FIG. 7. (a) The Fe-Fe interatomic exchange coupling parameters calculated for the FM (open circles) and AFM (open diamonds) FeRh compound with 1% substitution of Rh by Fe atoms: one Fe atom belongs to the Fe sublattice, and another one to the Rh sublattice.

DLM approach by Staunton *et al.* [12], that leads, however, to much more time-consuming calculations of the temperature dependent properties.

IV. SUMMARY

To summarize, we have studied here the AFM-FM metamagnetic transition in FeRh on the basis of the first-principles DFT calculations. The temperature dependent stability of these phases was investigated performing total energy calculations for the systems with a different degree of magnetic disorder treated within the uDLM approach. The first-principles calculations supply in addition the parameters (element projected magnetic moments, exchange coupling parameters) for the extended Heisenberg model Eq. (2). Based on this Hamiltonian, Monte Carlo simulations have been performed. The results of both calculations allow to identify the crucial role and interplay of two factors: (i) the dependence of the Fe-Fe exchange coupling parameters on the temperature-governed degree of magnetic disorder in the system; (ii) the Rh induced magnetic

moment, also dependent on the magnetic disorder in the system, that stabilize the FM state. An important observation is the competing effect of the temperature dependence of these two factors. Increase of disorder for rising temperature leads to a decrease of the Rh magnetic moments and as a result to a decrease of Fe-(Rh)-Fe FM exchange interactions responsible for lowering the energy of the FM state. On the other hand, the decrease of the AFM Fe-Fe $\bar{J}_{ij}^{\text{Fe-Fe}}(\bar{m})$ exchange interactions [see extended Hamiltonian Eq. (2) together with the temperature induced magnetic disorder leads to a stabilization of the FM state]. Suppressing the interplay of these two effects leads to a shift of the point of metamagnetic transition. This was demonstrated by studying the impact of impurities either on the Fe or on the Rh sublattices.

ACKNOWLEDGMENTS

We thank Dr. M. Grüner for helpful discussions and the DPG for financial support via SFB 689 (Spinphänomene in reduzierten Dimensionen).

-
- [1] J. S. Kouvel and C. C. Hartelius, *J. Appl. Phys.* **33**, 1343 (1962).
 [2] S. Maat, J.-U. Thiele, and E. E. Fullerton, *Phys. Rev. B* **72**, 214432 (2005).
 [3] C. Stamm, J.-U. Thiele, T. Kachel, I. Radu, P. Ramm, M. Košuth, J. Minár, H. Ebert, H. A. Dürr, W. Eberhardt, and C. H. Back, *Phys. Rev. B* **77**, 184401 (2008).
 [4] E. Mancini, F. Pressacco, M. Haertinger, E. E. Fullerton, T. Suzuki, G. Woltersdorf, and C. H. Back, *J. Phys. D* **46**, 245302 (2013).
 [5] M. E. Gruner, E. Hoffmann, and P. Entel, *Phys. Rev. B* **67**, 064415 (2003).
 [6] R. Y. Gu and V. P. Antropov, *Phys. Rev. B* **72**, 012403 (2005).
 [7] L. M. Sandratskii and P. Mavropoulos, *Phys. Rev. B* **83**, 174408 (2011).
 [8] P. M. Derlet, *Phys. Rev. B* **85**, 174431 (2012).
 [9] V. L. Moruzzi and P. M. Marcus, *Phys. Rev. B* **46**, 14198 (1992).
 [10] O. N. Mryasov, *Phase Transitions* **78**, 197 (2005).
 [11] J. Barker and R. W. Chantrell, *Phys. Rev. B* **92**, 094402 (2015).
 [12] J. B. Staunton, R. Banerjee, M. dos Santos Dias, A. Deak, and L. Szunyogh, *Phys. Rev. B* **89**, 054427 (2014).
 [13] J. Kudrnovský, V. Drchal, and I. Turek, *Phys. Rev. B* **91**, 014435 (2015).
 [14] C. Kittel, *Phys. Rev.* **120**, 335 (1960).
 [15] J. S. Kouvel, *J. Appl. Phys.* **37**, 1257 (1966).
 [16] M. P. Annaorazov, S. A. Nikitin, A. L. Tyurin, K. A. Asatryan, and A. K. Dovletov, *J. Appl. Phys.* **79**, 1689 (1996).
 [17] P. Tu, A. J. Heeger, J. S. Kouvel, and J. B. Comly, *J. Appl. Phys.* **40**, 1368 (1969).
 [18] J. B. McKinnon, D. Melville, and E. W. Lee, *J. Phys. C* **3**, S46 (1970).
 [19] P. H. L. Walter, *J. Appl. Phys.* **35**, 938 (1964).
 [20] R. Barua, F. Jimnez-Villacorta, and L. H. Lewis, *Appl. Phys. Lett.* **103**, 102407 (2013).
 [21] W. Lu, N. T. Nam, and T. Suzuki, *J. Appl. Phys.* **105**, 07A904 (2009).
 [22] C. Brouder and K. H. Bennemann, *Physica B* **208-209**, 73 (1995).
 [23] Y. Kobayashi, K. Muta, and K. Asai, *J. Phys. Condens. Matter* **13**, 3335 (2001).
 [24] H. Ebert *et al.*, The Munich SPR-KKR package, version 6.3: H. Ebert *et al.* <http://olymp.cup.uni-muenchen.de/ak/ebert/SPRKKR>, 2012.
 [25] H. Ebert, D. Ködderitzsch, and J. Minár, *Rep. Prog. Phys.* **74**, 096501 (2011).
 [26] J. P. Perdew, K. Burke, and M. Ernzerhof, *Phys. Rev. Lett.* **77**, 3865 (1996).
 [27] J. Kudrnovský, V. Drchal, I. Turek, and P. Weinberger, *Phys. Rev. B* **78**, 054441 (2008).
 [28] K. Binder, *Rep. Prog. Phys.* **60**, 487 (1997).
 [29] D. P. Landau and K. Binder, *A Guide to Monte Carlo Simulations in Statistical Physics* (Cambridge University Press, Cambridge, 2000).
 [30] A. I. Liechtenstein, M. I. Katsnelson, and V. A. Gubanov, *J. Phys. F: Met. Phys.* **14**, L125 (1984).
 [31] A. I. Liechtenstein, M. I. Katsnelson, V. P. Antropov, and V. A. Gubanov, *J. Magn. Magn. Mater.* **67**, 65 (1987).
 [32] A. Deák, E. Simon, L. Balogh, L. Szunyogh, M. dos Santos Dias, and J. B. Staunton, *Phys. Rev. B* **89**, 224401 (2014).
 [33] G. Shirane, R. Nathans, and C. W. Chen, *Phys. Rev.* **134**, A1547 (1964).
 [34] E. Müller-Hartmann, U. Kbler, and L. Smardz, *J. Magn. Magn. Mater.* **173**, 133 (1997).
 [35] S. Shallcross, A. E. Kissavos, V. Meded, and A. V. Ruban, *Phys. Rev. B* **72**, 104437 (2005).
 [36] S. Shallcross, A. E. Kissavos, S. Sharma, and V. Meded, *Phys. Rev. B* **73**, 104443 (2006).
 [37] B. L. Gyorffy, A. J. Pindor, J. Staunton, G. M. Stocks, and H. Winter, *J. Phys. F: Met. Phys.* **15**, 1337 (1985).
 [38] S. Polesya, S. Mankovsky, O. Šipr, W. Meindl, C. Strunk, and H. Ebert, *Phys. Rev. B* **82**, 214409 (2010).
 [39] C. Baldasseroni, C. Bordel, C. Antonakos, A. Scholl, K. H. Stone, J. B. Kortright, and F. Hellman, *J. Phys. Condens. Matter* **27**, 256001 (2015).